Photoemission studies of As_xSe_{100-x} (x: 0, 50, 100) films prepared by pulsed-laser deposition—the effect of annealing

2006 J. Phys.: Condens. Matter 18 5525

(http://iopscience.iop.org/0953-8984/18/23/022)

INSTITUTE OF PHYSICS PUBLISHING JOURNAL OF PHYSICS: CONDENSED MATTER

J. Phys.: Condens. Matter **18** (2006) 5525–5534 doi:10.1088/0953-8984/18/23/022

Photoemission studies of As_xSe_{100-x} (x: 0, 50, 100) films prepared by pulsed-laser deposition—the effect of annealing

A Siokou[1], M Kalyva[1,2], S N Yannopoulos[1], M Frumar[3] and P Němec[3]

[1] Foundation of Research and Technology Hellas-Institute of Chemical Engineering and High Temperature Chemical Processes (FORTH/ICE-HT), PO Box 1414, GR-26504, Rio, Patras, Greece
[2] Department of Chemical Engineering, University of Patras, GR-26504, Patras, Rio, Greece
[3] Department of General and Inorganic Chemistry and Research Center, University of Pardubice, Legions Square 565, Pardubice 53210, Czech Republic

E-mail: siokou@iceht.forth.gr

Received 9 February 2006
Published 26 May 2006
Online at stacks.iop.org/JPhysCM/18/5525

Abstract

Annealing-induced structural changes in amorphous films As_xSe_{100-x} (x: 0, 50, 100) prepared by pulsed laser deposition (PLD) on Si substrates were studied by x-ray and ultraviolet photoelectron spectroscopies (XPS, UPS). For $x = 50$, the analysis of the XPS As 3d peak revealed three distinct local environments in which the As atoms participate in the as-prepared films. The combination of photoemission and work function measurements showed that annealing close to the glass transition temperature induces atomic rearrangements towards the formation of a more homogenous surface composition as well as to a more energetically favoured film structure, by cleavage of the weaker As–As and Se–Se bonds towards the formation of As–Se ones analogously to As–S system films.

1. Introduction

Binary chalcogenide glasses of the form M_xCh_{100-x} can be prepared in a wide range of compositions [1, 2]; Ch denotes a chalcogen atom (S, Se, Te) and M is usually one of the atoms As, Sb, Ge. Bulk chalcogenide glasses are relatively easy to prepare up to the stoichiometric composition, e.g. for $x = 33$ in tetrahedral glasses (Ge), and for $x = 40$ in glasses favouring pyramidal units (As and Sb). When exceeding the above x values, the glass formation becomes more difficult, requiring higher quenching rates. Therefore, amorphous films of the desired compositions can be prepared by thermal evaporation and sputtering techniques. The interest in high x compositions, e.g. $x = 50$ in the As_xSe_{100-x} binary system, lies in the fact that the formation of such glasses implies the formation of homopolar As–As bonds, which are

important for a variety of photo-induced metastable effects [3] occurring upon near-bandgap light irradiation. The glasses with higher x possess higher index of refraction [4]. For example, the symmetric $As_{50}Se_{50}$ has been in the focus of many investigations; one of them demonstrated the optomechanical effect [5]. This is among the many interesting photo-induced effects, which render chalcogenide glasses ideally suitable media for many important applications (such as optical gratings, microlenses, holographic media, optical memories, nonlinear optical elements, bio- and electrochemical sensors, and photoresists) [3, 4, 6–8].

Film fabrication can alternatively be achieved by pulsed laser deposition (PLD). This method is considered as more suitable compared with the classical deposition techniques mentioned above, having the advantage of maintaining quite well the composition of the target material in the structure of the films [9]. Moreover, using PLD one can avoid the formation of columnar structures and structural heterogeneity that sometimes emerge from the thermal evaporation method. Thus PLD implies a different type of building of the amorphous structure, which in turn can lead to a milder response of the film to some external stimulus (e.g. irradiation, annealing, etc). Nevertheless, only a few papers deal with amorphous chalcogenide thin films prepared by PLD (see, e.g. [6, 7, 10] and papers mentioned). Further, structural studies of amorphous chalcogenides have been mainly conducted with the aid of vibrational spectroscopy [6, 8, 11]. On the other hand, experimental studies on electronic structure elucidation with surface-sensitive techniques are rather sporadic, whilst theoretical calculations on electronic structure are frequently employed to enlighten structural modifications in such systems [12]. A brief survey of such studies will be presented below in order to facilitate the subsequent discussion.

The valence band (VB) features of a series of *thermally evaporated* a-As_xSe_{1-x} films have been studied by Hayashi *et al* using ultraviolet photoelectron spectroscopy (UPS) and inverse photoemission spectroscopies (IPES) [13]. It was found that changes in the UPS and IPES spectral features occur at $x \geqslant 0.4$ and they attributed them to the percolation of $As(Se_{1/2})_3$ units over the material, in agreement with the predictions of the Phillips–Thorpe rigidity percolation theory [14]. High-resolution XPS was used by Jain *et al* [15] for the investigation of light-induced changes in $As_{50}Se_{50}$ films prepared by *thermal evaporation*. These studies revealed that illumination by a He–Ne laser (1.96 eV) caused a permanent enrichment of the surface with Se and a transformation of a fraction of As–As bonds into As–Se bonds; the latter leads to a more homogenous chemical environment for As. Similar effects were found for the As–S system [8]. Reversible photo-induced changes were also observed in the bulk glasses, including transformation of the lone pair (LP) electrons of Se into more tightly bound states. Li *et al* [16] reported an interpretation of the observed structures of the XPS valence band spectra of g-As_4Se_4, by examining the charge distribution of states in a main building block As–$AsSe_2$. They attributed the three groups of peaks of these spectra, at binding energy (BE) ∼4.9, 2.9, 1.4 eV, to the intra-building, inter-building block bonds and LP, respectively. Since any light-induced structural change is likely to involve bond changes and formation in or between different building blocks (intra- and inter-molecular building blocks, respectively), the above assignment helps to explain the photoresponse observed experimentally in a-As_4Se_4 films. Krishnaswami *et al* [17] found a depletion of states in the inter-building block region as a result of the *in situ* irradiation of a-As_4Se_4 films in air, which was explained as a light-induced reduction of the number of As–As bonds and reaction with oxygen.

The absence of systematic studies on the effect of annealing on the electronic structure of amorphous chalcogenides and especially of *pulsed laser deposited* films led us to undertake the present study. Amorphous As, Se and chalcogenide $As_{50}Se_{50}$ films were prepared by PLD on Si substrates and characterized by x-ray and UV–photoelectron spectroscopies. The study focuses on the annealing-induced changes in the surface electronic properties of the above films.

2. Experimental details

The amorphous thin films of As_xSe_{100-x} (x: 0, 50, 100) were prepared by PLD using rotating targets of As, Se and chalcogenide glasses with nominal composition of As_4Se_4. The target glasses were prepared by the conventional melt–quenching method. A KrF excimer laser (LAMBDA PHYSIK COMPex 102) operating at 248 nm with constant output energy of 300 mJ per pulse (pulse duration 30 ns and with repetition rate of 20 Hz) was used for the PLD of the amorphous films. The procedure has been described in detail elsewhere [18]. The composition of the as-deposited films was carefully controlled by x-ray fluorescence (XRF-EDX). In the case of the As–Se system, the differences between the chemical composition of the target material and of the films were found to be within experimental error (±1 at.%).

The photoemission experiments were carried out in a ultra-high-vacuum system, which consists of a fast entry specimen assembly, a sample preparation and an analysis chamber with a base pressure $<5 \times 10^{-10}$ mbar. The system is equipped with a hemispherical electron energy analyser (SPECS LH-10), a twin anode x-ray gun and a UV lamp for XPS and UPS measurements, respectively. The non-monochromatized Al Kα line at 1486.6 eV and analyser pass energy of 12 eV, giving a full width at half maximum (FWHM) of 0.9 eV for the Au $4f_{7/2}$ peak, were used in XPS measurements. The O 1s and C 1s XPS peaks were measured using a higher analyser pass energy (97 eV). Additional measurements were performed with the Mg Kα x-ray line ($h\nu = 1253.6$ eV). The XPS core level spectra were analysed by a fitting routine, which decomposes each spectrum into individual mixed Gaussian–Lorentzian peaks after a Shirley background subtraction. Usually the BE scale in XPS measurements is calibrated by assigning the main C 1s peak at 284.6 eV [19]. This was not possible for the present system because the C 1s peak overlaps with the Auger peaks Se (LMM) and As (LMM). Thus, the calibration of the binding energy scale was achieved using the XPS valence band spectra, by assigning the intersection of the background with the slope of the valence band to BE = 0 eV. UPS spectra were obtained using the HeI resonance line ($h\nu = 21.23$ eV). The work function ($e\Phi$) was determined for all the surfaces from the UPS spectra by subtracting their width (i.e. the energy difference between the analyser Fermi level and the high binding energy cut-off), from the HeI excitation energy (21.23 eV). For these measurements a bias of −12.23 V was applied to the sample in order to avoid interference of the spectrometer threshold in the UPS spectra. The samples were characterized before and after mild Ar^+ sputtering (3 kV, $I_{\text{sample}} = 3\ \mu$A, $t = 5$ min) which is necessary in order to obtain atomically clean surfaces and reproducible UPS spectra. All the UPS spectra presented here refer to sputtered surfaces.

The $As_{50}Se_{50}$ films were characterized in both the as-prepared state and the annealed states. During the annealing process the sample was placed in a tube filled with nitrogen (N_2) that was heated for 90 min at 150 °C. XPS and UPS studies were also performed for another film of the same composition, resulting in reproducible findings.

3. Results

3.1. XPS results

The XPS core level peaks Se 3d and As 3d, for the films with stoichiometry As_xSe_{100-x} (x: 0, 50, 100) before and after annealing, are shown in figures 1(a) and (b). The distinct peaks due to spin–orbit splitting (SOS) for the doublets originating from the Se 3d (SOS = 0.86 eV) and As 3d (SOS = 0.7 eV) core levels are not well resolved at the present instrumental energy resolution. For the analysis of these spectra, the fitting routine keeps the SOS of each component fixed to the above values and the FWHM of each peak ($3d_{5/2}$ and $3d_{3/2}$) in the doublets is also kept fixed (FWHM = 1 eV and 1.1 eV for Mg Kα and Al Kα respectively).

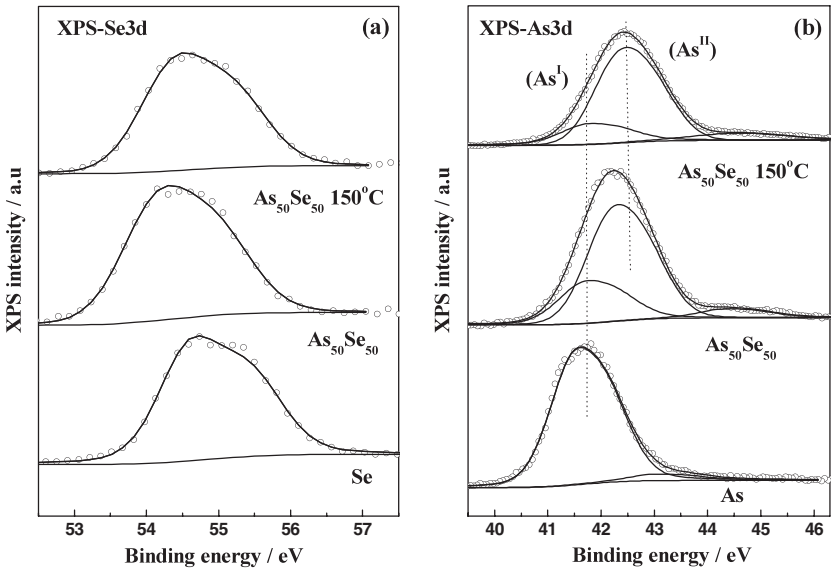

Figure 1. (a) Se 3d XPS peaks of the Se film (bottom spectrum) and of the $As_{50}Se_{50}$ as-prepared and annealed films (middle and top spectra). (b) As 3d XPS peaks of the As film (bottom spectrum) and of the $As_{50}Se_{50}$ as-prepared and annealed films (middle and top spectra).

Table 1. Binding energies of the Se 3d and As 3d XPS peaks of the as-prepared and annealed As, Se and $As_{50}Se_{50}$ (two samples denoted as #1 and #2) films. Contribution (%) of the As^{I} component to the total As 3d peak signal (f_{AsI}).

	As-prepared films				Annealed films			
	Se $3d_{5/2}$ BE/eV (±0.05)				Se $3d_{5/2}$ BE/eV (±0.05)			
Se	54.6							
$As_{50}Se_{50}$#1	54.2				54.4			
$As_{50}Se_{50}$#2	54.1				54.2			
	As $3d_{5/2}$ BE/eV (±0.05)			f_{AsI}	As $3d_{5/2}$ BE/eV (±0.05)			f_{AsI}
	As^{I}	As^{II}	As^{III}	(%)	As^{I}	As^{II}	As^{III}	(%)
As	41.6		43.8					
$As_{50}Se_{50}$#1 (Bef. sptr.)	41.6	42.2	44.3	12.9	41.6	42.2	44.2	7.8
$As_{50}Se_{50}$#1 (After sptr.)	41.6	42.1	44.5	28.5	41.6	42.2	44.7	20.6
$As_{50}Se_{50}$#2 (Bef. sptr.)	41.6	42.2	44.2	15.3	41.6	42.2	44.3	8.6
$As_{50}Se_{50}$#2 (After sptr.)	41.6	42.2	44.3	41.4	41.6	42.2	44.3	36.1

Each component of the analysed spectra shown in figure 1 is *the sum* of the $3d_{5/2}$ and $3d_{3/2}$ contributions. The BE values mentioned below refer to the $3d_{5/2}$ peak.

The Se 3d spectrum of the Se film, bottom spectrum in figure 1(a), consists of one doublet at BE = 54.6 eV (Se $3d_{5/2}$) which is the characteristic energy of elemental Se [15, 20]. The middle spectrum of figure 1(a) shows the Se 3d peak originating from the $As_{50}Se_{50}$ film that is detected at BE = 54.2 eV. The binding energy of the Se 3d XPS peak of the post-annealed $As_{50}Se_{50}$ film (top spectrum in figure 1(a)) has shifted to higher values by 0.2 eV as compared to the as-prepared samples. The BE values are listed in table 1.

The As 3d spectrum of the elemental As film, bottom spectrum in figure 1(b), consists of a main component (denoted as As^I) at BE = 41.6 eV (As $3d_{5/2}$) which is the characteristic energy of elemental As [15, 21] and a second peak (As^{III}) with very low intensity at 43.8 eV that represents oxidized As; since the films have not been prepared *in situ* the presence of small amounts of contamination on the surface is inevitable. The binding energy of the As 3d peak originating from As_2O_3 is reported in the literature at about 44.5 eV [22]. The lower BE detected here is attributed to arsenic atoms in sub-stoichiometric oxide (AsO_x). Assuming a uniform oxide layer on top of the As film, its thickness, d, can be calculated using a standard quantitative analysis procedure [19]. Such a calculation resulted in $d = 0.36$ nm, i.e. a value that is less than the thickness of one monolayer of As_2O_3 ($d_{ML} = 0.44$ nm).

The As 3d peak of the $As_{50}Se_{50}$ film exhibits three components, as illustrated in the middle spectrum of figure 1(b): one at high BE (As^{III}) that represents oxidized As, one at BE = 41.6 eV (As^I) that is characteristic of elemental As, and one at 42.1 eV (As^{II}). The BE of the As^{II} peak is in agreement with literature values reported for bulk a-As_2Se_3 [15] and for PLD As_2Se_3 films measured by our group [23]. The As 3d XPS peak of the post-annealed film (top spectrum of figure 1(b)) again exhibits three components (As^I, As^{II}, As^{III}) characterized by a different relative intensity ratio compared to the corresponding peaks of the as-prepared films.

In order to ascertain the accuracy of the XPS measurements, two $As_{50}Se_{50}$ films prepared under the same conditions were studied in the as-prepared and the annealed states. Table 1 tabulates the measured BEs of the As 3d and Se 3d peaks for the films studied in the present work before and after annealing, as well as the relative contribution (%) of the As^I component to the total As 3d peak area. The observed BEs for the two samples are the same within the limits of the experimental error (±0.05 eV).

Before sputtering of the $As_{50}Se_{50}$ film surface (see section 2), the O 1s peaks consist of two components: one at 533 eV and one at 531.3 eV. The former is characteristic of oxygen atoms of water molecules absorbed on the surface while the latter corresponds to oxygen atoms in As_2O_3 [22]. The existence of a mixed ($AsSeO_x$) surface oxide layer is not likely since the Se 3d peak exhibits no oxidation features. After sputtering only traces of the peak at 531.3 eV can be detected. At the same time, the As 3d spectrum shows that on the surface there still exists a small amount of oxidized arsenic.

The intensities of the As 3d and Se 3d XPS peaks corrected by the XPS atomic sensitivity factors (0.53 for As 3d and 0.67 for Se 3d) [19] were used in order to calculate the surface stoichiometry of the samples. The calculation was performed before and also after mild sputtering and the results are presented in table 2. It is well known that even mild ion bombardment may induce compositional changes in the surface region. This is clearly observed in the present case where the arsenic surface concentration of the films always increases after sputtering mainly due to preferential etching of selenium atoms. For this reason we presently discuss the behaviour of the As/Se atomic ratio before the sputtering procedure. When the Al Kα line is used the As/Se surface atomic ratio changes from the value 1.3 at the as-prepared state to As/Se = 1 after annealing. The latter is the nominal value for the $As_{50}Se_{50}$ compound. In the case of the Mg Kα line, the As/Se surface atomic ratio of the as-prepared film is found to be 0.85, a value significantly lower than the one measured using the Al Kα line, which becomes 0.94 after annealing. In both cases, the As content increases on the surface after sputtering probably due to preferential sputtering of the surface Se atoms.

3.2. UPS results

Valence band spectra of the as-prepared, $x = 0$, 50, 100, As_xSe_{100-x} films are presented in figure 2. As regards the spectrum of elemental Se, the peaks at 4.4 and 5.4 eV are characteristic

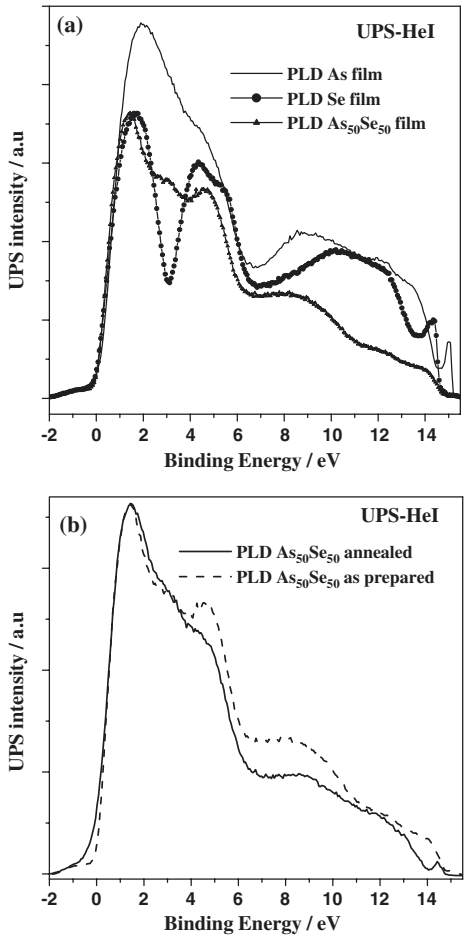

Figure 2. UPS-HeI spectra (a) of the As_xSe_{100-x} (x: 0, 50, 100) as-prepared films and (b) of the $As_{50}Se_{50}$ as-prepared and annealed films.

of 4p-like bonding electrons, while the peak at 10 eV is due to 4s electrons. The separation of the 4p-bonding peaks was attributed to the distortion of dihedral and bond angles on the Se chains [24]. The peak at 1.6 eV is characteristic of 4p-like lone pair (LP) electrons [25]. The spectrum of elemental As has a broad peak around 1.9 eV attributed to 4p-bonding electrons of As and a second one with lower intensity at 4.5 eV. The origin of the second peak is not quite clear in the literature. It has been attributed either to the reduced interaction between layers of the amorphous phase—as compared to the crystalline phase—or to the interaction of cyclic clusters of As atoms [26]. In the case of $As_{50}Se_{50}$, the UPS spectrum reveals peaks at 1.4 eV (LP electrons), 3.1 and 4.8 eV, where the latter are due to As–Se 4p-bonding electrons. The peak at 3.1 eV contains some contribution from As–As bonding while a small contribution of O 2p electrons at a binding energy of ∼5 eV cannot be excluded since traces of As_xO_y are detectable with XPS. Since the upper surface layer is expected to contain mainly $As_{50-x}Se_{50}$ and As_xO_y species, it is reasonable to consider that, due to the high surface sensitivity of UPS, the peak at 4.8 eV would include also some contribution from Se–Se 4p electrons. The peak at about 8 eV represents the 4s-bonding electrons [16]. Figure 2(b) shows the normalized UPS valence band spectra of the $As_{50}Se_{50}$ film before and after annealing. We observe that both the 4p-peak at 4.8 eV and the 4s-peak at ∼8 eV experience a decrease in their intensity after annealing.

Table 2. Surface atomic ratio (As/Se), of the as-prepared and annealed $As_{50}Se_{50}$ films, measured by Al Kα and Mg Kα x-ray lines before and after sputtering.

$As_{50}Se_{50}$	As/Se before sptr.	As/Se after sptr.
As-prepared		
Al Kα		
#1	1.3	1.6
#2	1.3	1.4
Mg Kα		
#1	0.85	1
Annealed		
Al Kα		
#1	1	1.6
#2	1	1.4
Mg Kα		
#1	0.94	1

Table 3. Work function (WF) values of the as-prepared and annealed As_xSe_{100-x} (x: 0, 50, 100) films.

	WF (eV) after sptr.
Se	5.4 (5.9 [27])
As	4.0 (4.6 [28])
As-prepared	
$As_{50}Se_{50}$#1	5.3
$As_{50}Se_{50}$#2	5.2
Annealed	
$As_{50}Se_{50}$#1	4.7
$As_{50}Se_{50}$#2	4.9

For each sample, the work function ($e\Phi$) of the surface was determined from the UV valence band spectrum and the error margin for these measurements is estimated to be ± 0.05 eV. The results that correspond to the sputtered samples are shown in table 3. The value of $e\Phi$ depends on the surface nature, morphology and composition. The values measured at the present experiments for the elemental a-As ($e\Phi = 4.0$ eV) and a-Se ($e\Phi = 5.4$ eV) films are lower than those reported in the literature for their crystalline counterparts that are $e\Phi_{\text{c-As}} = 4.6$ eV and $e\Phi_{\text{c-Se}} = 5.9$ eV [27, 28]. Further, the measured work function of the as-prepared $As_{50}Se_{50}$ film ($e\Phi = 5.3$ eV) lies closer to that of the α-Se film, while after annealing it shifts to lower values ($e\Phi = 4.7$–4.9 eV).

4. Discussion

It is well established [29] that for a film with $x = 0$, which corresponds to elemental Se, the glass structure is dominated by long, one-dimensional Se_n chains containing also a small fraction of Se_8 cyclic molecules, the ratio depending on the way of preparation. A quantification

of these two species has been recently achieved by Raman scattering experiments [30]. The addition of As causes a gradual knitting of the loosely interacting Se_n chains, which results in the formation of a network-like structure of low dimensionality. This process continues up to $x = 40$, where two-dimensional layers of $AsSe_{3/2}$ pyramids rings are formed [31]. At this point many physical properties of the binary system, such as the glass forming ability, the glass transition temperature and the shear modulus, are maximized [1, 2]. Interesting effects occur upon a further increase of As atoms where closed cage-like species start forming. At the symmetric composition, $x = 50$, besides the glass, there exists a stable crystalline form similar to the realgar of the corresponding sulfide alloy.

Raman studies have shown that the structure of As_xSe_{100-x} PLD films with $x \geqslant 40$ probably contain $AsAs_{3-n}Se_n$ ($n = 0, 1, 2, 3$) structural units while molecular-like species such as As_kSe_m ($k = 4$, $m = 4$ and $k = 4$, $m = 5$) are found at concentrations even lower than those found in the corresponding bulk glasses [18]. As has been shown in our previous work [23], these four different $AsAs_{3-n}Se_n$ species result in two distinct As 3d XPS peaks, denoted as As^{I} and As^{II}, that contain the unresolved contributions of the $n = 0, 1, 2, 3$ units. As_4 and As_3Se units form the As^{I} or *elemental-like* arsenic domains while $AsSe_3$ and probably also $(As_2Se_2)_2$ form the As^{II} or *stoichiometric-like* domains.

The surface of the as-prepared samples seems to be rich in As (As/Se = 1.3) when measured by the Al Kα x-ray line while the opposite is observed with the Mg Kα line (As/Se = 0.85). The reason for this discrepancy on the XPS determined surface composition can be attributed to the energy difference between the Mg and Al anodes ($\Delta E = 233$ eV) which leads to differences in the As 3d and Se 3d photoelectron escape depths. Similar discrepancies have been observed earlier by Burns *et al* [32] on $As_{50}Se_{50}$ films deposited by RF sputtering on SiO_2 substrates. The calculated inelastic mean free paths (λ) for the As 3d and Se 3d photoelectrons through an As_xSe_{1-x} matrix are $\lambda_{As\ 3d} \approx \lambda_{Se\ 3d} = 3.64$ nm and $\lambda_{As\ 3d} \approx \lambda_{Se\ 3d} = 3.34$ nm for Al Kα and Mg Kα respectively [19]. This difference reflects a slightly enhanced surface sensitivity of the Mg Kα line, in other words the topmost surface layers would have more 'weight' in the total As and Se intensities in the case of Mg Kα excitation. According to the As 3d spectra analysis the uppermost surface layer of the samples consists of $As_{50-x}Se_{50}$ units and oxidized arsenic (As_xO_y). Throughout the measurements partial desorption of the oxide leads to a depletion of arsenic at the surface which is reflected at the low As/Se ratio measured by the Mg Kα line. This is also reflected by the relatively high $e\Phi$ value of the as-prepared films. Work function measurements of $As_{50}Se_{50}$ films exposed to oxidative atmosphere have shown that the $e\Phi$ value rises as the surface becomes more oxidized. A value of $e\Phi = 6$ eV, for example, has been measured for a film covered with two monolayers of As_2O_3. This fact in combination with the excess of Se on the surface justifies the high $e\Phi$ value of the as-prepared films.

On the other hand the surface composition measured by the Al Kα line indicates that, despite the As deficiency of the upper layer, the surface region of the film ($\sim$10 nm) is enriched with arsenic. This has been previously observed by Jain *et al* [14] on thermally evaporated $As_{50}Se_{50}$ films. The analysis of the As 3d spectrum in the present work shows that about 30% of it corresponds to arsenic embedded in a matrix whose structure resembles that of the elemental arsenic (As^{I} or elemental-like) and about 5–10% to oxidized arsenic.

Annealing of the film reduces the amount of elemental-like arsenic from the surface region and the As/Se atomic ratio is now equal to 1 and 0.94 when measured by Al Kα and Mg Kα, respectively. These values are close or equal to the nominal one and this time no large discrepancy between the two measurements is observed, indicating that an atomic rearrangement has taken place leading to a more homogenous surface composition. The lower work function (4.7–4.9 eV) of the annealed films, lying almost in the middle between the two

extreme values measured for a-Se and a-As, indicates that the surface area of the annealed films has a composition that is closer to the nominal one as compared to that of the as-prepared films. The observed changes in the composition of the film upon annealing can be related to segregation of selenium towards the surface in order to lower the surface energy. The surface energy γ of arsenic in its bulk state ($\gamma = 45$ eV Å^{-2}) has been calculated by Moll *et al* [33]. Although, to our knowledge, no absolute γ value has been reported for pure selenium, recent theoretical calculations using density functional methods [34, 35] have shown that its value is generally lower than that of pure arsenic. Depletion of stoichiometric-like arsenic from the surface region is thus expected to lead to a more thermodynamically stable surface.

The valence band spectrum obtained by UP reveals a depletion of the peak attributed to As–As 4s bonding electrons (BE $\sim$ 8 eV), indicating that annealing of the sample causes the interaction of As–As bonds with Se and the decrease of their density. The effect is probably analogous to the one in the As–S system [8]. Another significant change in the UPS spectrum after annealing is the intensity decrease of the peak attributed to 4p electrons of the As–Se and Se–Se bonds or O 2p electrons at BE $\sim$ 4.8–5 eV. The reason for this can be the fact that the sample at this stage has less surface oxygen as compared to that before annealing (top spectra in figures 2(a) and (b)) while the breaking of Se–Se bonds and the formation of As–Se bonds cannot be excluded.

The effect of annealing on the electronic structure of amorphous chalcogenide PLD As_xSe_{100-x} (x: 40, 60, 70) films has been previously investigated by XPS [20]. On general grounds, annealing is expected to lower the internal energy of the amorphous state. At the intermediate compositions ($x = 50$–60) the as-prepared film structure is presumably composed of all the different structural units of $AsAs_{3-n}Se_n$ ($n = 0, 1, 2, 3$). At this composition, units with $n = 0, 1, 3$ are not energetically favoured and by annealing they will tend to transform to $(As_2Se_2)_2$ units. Indeed the lowest energy form of this composition (crystalline As_4Se_4) is composed of $(As_2Se_2)_2$ cage-like molecules. These changes are detected by XPS as a decrease of the elemental-like (As^{I}) component and as an increase of the stoichiometric-like (As^{II}) ones ($AsSe_3$ pyramids), while changes in the UPS spectra involve the intensity decrease of the bands attributed to As–As and Se–Se 4s and 4p bonding states. In conclusion, XPS and UPS measurements show that annealing of the $As_{50}Se_{50}$ film close to the T_g may cause a similar effect as irradiation: it reduces primarily a number of weaker As–As and Se–Se homopolar bonds [E(As–As) = 200 kJ mol^{-1} < E(Se–Se) = 225 kJ mol^{-1} < E(As–Se) = 230 kJ mol^{-1}] [36], causing the formation of As–Se heteropolar bonds.

5. Conclusions

Amorphous films with composition As_xSe_{100-x} (x: 0, 50, 100) were prepared by pulsed laser deposition on Si substrates. Annealing-induced changes in the surface electronic properties of the films were investigated using x-ray and ultraviolet photoelectron spectroscopies. The analysis of the XPS As 3d peaks revealed three distinct local environments in which the As atoms participate. It was shown that annealing the $As_{50}Se_{50}$ film close to the T_g causes atomic rearrangements by cleavage of the weaker As–As and Se–Se bonds towards the formation of As–Se ones analogously to As–S system films.

Acknowledgments

The Greek side acknowledges financial support from the General Secretariat for Research and Technology–Hellas in the framework of the bilateral project GR-CZ (2003–2005) and the program PENED 2003 (03EΔ887) in collaboration with O.T.E. SA. The Czech side

acknowledges financial support through the programs KONTAKT ME 690 and LC 523 of Ministry of Education and Youth of the Czech Republic.

References

[1] Elliott S R 1990 *Physics of Amorphous Materials* 2nd edn (London: Longman Scientific)
[2] Feltz A 1993 *Amorphous Inorganic Materials and Glasses* (Weinheim: VCH)
[3] Kolobov A V 2003 *Photo-induced Metastability in Amorphous Semiconductors* (Berlin: Wiley–VCH)
Kolobov A V and Tanaka K 2001 *Handbook of Advanced Electronic and Photonic Materials and Devices* vol 5 *Chalcogenide Glasses and Sol–Gel Materials* ed H S Nalwa (New York: Academic) pp 47–90
[4] Frumar M, Jedelsky J, Frumarova B, Wagner T and Hrdlicka M 2003 Optically and thermally induced changes of structure, linear and non-linear optical properties of chalcogenide thin films *J. Non-Cryst. Solids* **326–327** 399–404
[5] Krecmer P, Moulin A M, Stephenson R J, Rayment T, Welland M E and Elliott S R 1997 *Science* **277** 1799
[6] Frumar M, Nemec P, Frumarova B and Wagner T 2005 Pulsed laser ablation and deposition of chalcogenide thin films *Pulsed Laser Deposition of Optoelectronics Films* ed M Popescu (Bucuresti: INOE Publ House) pp 81–120
[7] Frumar M, Frumarova B, Nemec P, Wagner T, Jedelsky J and Hrdlicka M 2006 Thin chalcogenide films prepared by pulsed laser deposition—new amorphous materials applicable in optoelectronics, chemistry and biology *J. Non-Cryst. Solids* at press
[8] Frumar M, Frumarova B, Wagner T and Nemec P 2003 Photoinduced phenomena in amorphous and glassy chalcogenides *Photoinduced Metastability in Amorphous Semiconductors* ed A Kolobov (Weinheim: Wiley–VCH) pp 23–44
[9] Nemec P, Jedelsky J, Frumar M, Stabl M and Vlcek M 2004 *J. Phys. Chem.* **65** 1253–8
[10] Nemec P and Frumar M 2003 *J. Optoelectron. Adv. Mater.* **5** 1047–58
[11] See for example in Kolobov A V 2003 *Photo-induced Metastability in Amorphous Semiconductors* (Berlin: Wiley–VCH) chapters 2 and 8
[12] Drabold D A, Biswas P, Tafen D and Atta-Fynn R 2004 *Non-Crystalline Materials for Optoelectronics* ed G Lucovsky and M Popescu (Bucharest: INOE) pp 441–67
see also Kolobov A V 2003 *Photo-induced Metastability in Amorphous Semiconductors* (Berlin: Wiley–VCH) chapter 15
[13] Hayashi Y, Sato H and Taniguchi M 1999 *J. Electron Spectrosc.* **101–103** 681–4
[14] Phillips J C and Thorpe M F 1985 *Solid State Commun.* **53** 699
[15] Jain H, Krishnaswami S, Miller A C, Krecmer P, Elliott S R and Vlcek M 2000 *J. Non-Cryst. Solids* **274** 115–23
[16] Li J and Drabold D A 2002 *Phys. Rev. Lett.* **88** 2785
[17] Krishnaswami S, Jain H and Miller A C 2000 *J. Optoelectron. Adv. Mater.* **3** 695–702
[18] Nemec P, Jedelsky J, Frumar M, Stabl M and Vlcek M 2004 *J. Phys. Chem. Solids* **65** 1253
Nemec P, Jedelsky J, Frumar M, Stabl M and Cernosek Z 2005 *Thin Solid Films* **484** 140
[19] Briggs D and Seah M P 1990 *Practical Surface Analysis* 2nd edn (England: Wiley)
[20] Miyake I, Tanpo T and Tatsuyama C 1984 *J. Appl. Phys.* **23** 172
[21] Mårtensson N, Reihl B and Vogt O 1982 *Phys. Rev.* B **25** 824
[22] Barr T L, Hoppe E, Dugall T, Shah P and Seal S 1999 *J. Electron Spectrosc.* **95** 98–9
[23] Siokou A, Kalyva M, Yannopoulos S N, Němec P and Frumar M 2006 *J. Non-Cryst. Solids* at press
[24] Takahashi T, Ohno K and Harada Y 1980 *Phys. Rev.* B **8** 21
[25] Takahashi T and Sagawa T 1982 *Phys. Rev.* B **12** 26
[26] Takahashi T and Harada Y 1981 *Phys. Rev.* B **6** 24
[27] Johanson Robert E, Kasap S O, Rowlands J and Polischuk B 1998 *J. Non-Cryst. Solids* **227–230** 1359–62
[28] Taft E and Apker L 1949 *Phys. Rev.* B **75** 1181
[29] Gerlach E and Grosse P 1979 *The Physics of Selenium and Tellurium* (New York: Springer)
[30] Yannopoulos S N and Andrikopoulos K S 2004 *J. Chem. Phys.* **121** 4747–58
[31] Zallen R 1983 *Physics of Amorphous Solids* (New York: Wiley)
[32] Bruns M, Klewe-Nebenius H, Pfennig G, Bychkov E and Ache H J 1997 *Surf. Coat. Technol.* **97** 707–12
[33] Moll N, Kley A, Pehlke E and Scheffler M 1996 *Phys. Rev.* B **54** 8844–55
[34] Gundel S and Faschinger W 1999 *Phys. Rev.* B **59** 5602–11
[35] González C, Benito I, Ortega J, Jurczyszyn L, Blanco J M, Perez R, Flores F, Kampen T U, Zahn D R T and Braun W 2004 *J. Phys.: Condens. Matter* **16** 2187–206
[36] Popescu M A 2000 *Non-Crystalline Chalcogenides* (Dordrecht: Kluwer–Academic)